

1 **SM2RAIN-ASCAT (2007-2018): global daily satellite rainfall**
2 **from ASCAT soil moisture**

3

4 Luca Brocca^{1*}, Paolo Filippucci¹, Sebastian Hahn², Luca Ciabatta¹, Christian Massari¹,
5 Stefania Camici¹, Lothar Schüller³, Bojan Bojkov³, Wolfgang Wagner²

6

7

8 [1]{Research Institute for Geo-Hydrological Protection, National Research Council, Perugia, Italy}

9 [2]{Department of Geodesy and Geoinformation, Vienna University of Technology, Vienna, Austria }

10 [3]{European Organisation for the Exploitation of Meteorological Satellites, Darmstadt, Germany }

11

12

13

14

15

16

17

18

19

August 2019

20

Re-Submitted to: *Earth System Science Data*

21

* Correspondence to: Ph.D. Luca Brocca, Research Institute for Geo-Hydrological Protection, National Research Council, Via della Madonna Alta 126, 06128 Perugia, Italy. Tel: +39 0755014418 Fax: +39 0755014420 E-mail: luca.brocca@irpi.cnr.it.

22 **Abstract**

23 Long-term gridded precipitation products are crucial for several applications in
24 hydrology, agriculture and climate sciences. Currently available precipitation products suffer
25 from space and time inconsistency due to non-uniform density of ground networks and the
26 difficulties in merging multiple satellite sensors. The recent “bottom up” approach that exploits
27 satellite soil moisture observations for estimating rainfall through the SM2RAIN algorithm is
28 suited to build consistent rainfall data record as a single polar orbiting satellite sensor is used.

29 We exploit here the Advanced SCATterometer (ASCAT) on board three Metop satellites,
30 launched in 2006, 2012 and 2018, as part of the EUMETSAT Polar System programme. The
31 continuity of the scatterometer sensor is ensured until mid-2040s through the Metop Second
32 Generation Programme. Therefore, by applying SM2RAIN algorithm to ASCAT soil moisture
33 observations, a long-term rainfall data record will be obtained, starting in 2007 until mid-2040s.
34 The paper describes the recent improvements in data pre-processing, SM2RAIN algorithm
35 formulation, and data post-processing for obtaining the SM2RAIN-ASCAT quasi-global (only
36 over land) daily rainfall data record at 12.5 km sampling from 2007 to 2018. The quality of
37 SM2RAIN-ASCAT data record is assessed on a regional scale through the comparison with
38 high-quality ground networks in Europe, United States, India and Australia. Moreover, an
39 assessment on a global scale is provided by using the Triple Collocation technique allowing us
40 also the comparison with the latest ECMWF reanalysis (ERA5), the Early Run version of the
41 Integrated Multi-Satellite Retrievals for Global Precipitation Measurement (IMERG), and the
42 gauge-based Global Precipitation Climatology Centre (GPCC) products.

43 Results show that the SM2RAIN-ASCAT rainfall data record performs relatively well
44 both at regional and global scale, mainly in terms of root mean square error when compared to
45 other products. Specifically, SM2RAIN-ASCAT data record provides performance better than
46 IMERG and GPCC in the data scarce regions of the world, such as Africa and South America.
47 In these areas, we expect the larger benefits in using SM2RAIN-ASCAT for hydrological and
48 agricultural applications. Limitations of SM2RAIN-ASCAT data record consist in the
49 underestimation of peak rainfall events and in the presence of spurious rainfall events due to
50 high frequency soil moisture fluctuations that might be corrected in the future with more
51 advanced bias correction techniques.

52 The SM2RAIN-ASCAT data record is freely available at
53 <https://doi.org/10.5281/zenodo.2591215>.

54 *Keywords:* Rainfall, Soil moisture, ASCAT, SM2RAIN, Remote Sensing.

55 **1 Introduction**

56 Rainfall is ranked the first among the Essential Climate Variable by the Global Climate
57 Observing System (GCOS) as it represents the most important variable in many applications in
58 geosciences (Maggioni and Massari, 2018). Long-term rainfall records are essential for drought
59 monitoring (e.g., Forootan et al., 2019), water resources management (e.g., Abera et al., 2017)
60 and climate studies (e.g., Herold et al., 2016; Pendergrass and Knutti, 2018) while near real-
61 time rainfall data are needed for the mitigation of the impacts of natural disasters such as floods
62 and landslides (e.g., Wang et al., 2107; Camici et al., 2018; Brunetti et al., 2018; Kirschbaum
63 and Stanley, 2018). Additional applications in which near real-time rainfall plays a crucial role
64 are weather forecasting, agricultural planning, vector-borne and waterborne diseases (e.g.,
65 Rinaldo et al., 2012; Thaler et al., 2018).

66 Three different techniques can be used for estimating rainfall: ground measurements,
67 meteorological modelling and remote sensing. Ground measurements are based on rain gauges
68 and meteorological radars (Lanza et al., 2009), but also new approaches such as microwave
69 links are being developed (e.g., Overeem et al., 2011). These measurements guarantee high
70 accuracy but suffer in many regions from limited spatial coverage (Kidd et al., 2017).
71 Alternatively, meteorological models are used to estimate rainfall mainly in areas without
72 ground reliable observations (Ebert et al., 2007), e.g., reanalysis. The uncertainties associated
73 with these estimates can be large, mainly in areas where ground observations are scarce
74 (Massari et al., 2017a). Therefore, to fill the gaps in the spatial coverage of ground
75 measurements, and to improve the estimates obtained by models, different remote sensing
76 techniques have been developed in the last 30 years (Hou et al., 2014). The standard methods
77 for estimating rainfall from space are based on instantaneous measurements obtained from
78 microwave radiometers, radars, and infrared sensors (Kidd and Levizzani, 2011). These
79 methods are based on inversion techniques where the upwelling radiation (or backscattered
80 signal for radars) is related to the surface precipitation rate, i.e., a “top down” approach (Brocca
81 et al., 2014).

82 The most recent and successful example of satellite precipitation estimates is represented
83 by the Integrated Multi-Satellite Retrievals for Global Precipitation Measurement, GPM
84 (IMERG) of the GPM mission (Hou et al., 2014) which provide high spatial (0.1°) and temporal

85 (30-minute) resolution and quasi-global coverage ($\pm 60^\circ$). To obtain such resolution and
86 coverage, the IMERG products use a constellation of polar and geostationary satellite sensors
87 operating in the microwave and infrared bands. However, the use of multiple sensors has some
88 problems, including: the inconsistency between rainfall estimates from different sensors
89 (intercalibration problem), the difficulties in collecting observations from multiple space
90 agencies (i.e., problem of delivering the products in near real-time), and the high costs for the
91 operation and the maintenance of the overall constellation. Moreover, as the top down approach
92 requires the merging of instantaneous rainfall measurements from multiple sensors, the failure
93 of one of them may imply a significant degradation in the accuracy of accumulated rainfall
94 estimate due to the high temporal variability of rainfall (Trenberth and Asrar, 2014).

95 In recent years, a new “bottom up” approach has emerged that uses satellite soil moisture
96 observations to infer, or to correct, rainfall over land (Brocca et al., 2013a; Crow et al., 2009;
97 Pellarin et al., 2013; Wanders et al., 2015). The major difference between the bottom up and
98 top down approaches is in the type of measurement; i.e., accumulated rainfall with the bottom
99 up method and instantaneous rainfall rates with the top down method. This difference makes
100 the two approaches highly complementary and their integration has been already successfully
101 tested and demonstrated in several recent studies (e.g., Brocca et al., 2016; Ciabatta et al., 2017;
102 Chiaravallotti et al., 2018; Massari et al. 2019). When accumulated rainfall estimates are needed
103 (e.g., daily rainfall), the bottom up approach has the advantage of requiring a much lower
104 number of measurements and, hence, of satellite sensors. The limitations of the bottom up
105 approach are the possibility to estimate only terrestrial rainfall and its dependence on land
106 characteristics (e.g., low accuracy for dense vegetation coverage and complex topography,
107 Brocca et al., 2014).

108 The bottom up approach has been applied over a range of scales: global (Crow et al.,
109 2011; Brocca et al., 2014; Ciabatta et al., 2018), continental (Wanders et al., 2015; Brocca et
110 al., 2016), and local (Massari et al., 2014; Brocca et al., 2015; Román-Cascón et al., 2017) scale.
111 Moreover, different satellite soil moisture products have been considered including SMOS (Soil
112 Moisture Ocean Salinity mission, Brocca et al., 2016), ASCAT (Advanced SCATterometer,
113 Brocca et al., 2017), AMSR-E (Advanced Microwave Scanning Radiometer, Crow et al., 2009),
114 and SMAP (Soil Moisture Active and Passive, Koster et al., 2016; Tarpanelli et al., 2017; Zhang
115 et al., 2019). First studies employing satellite rainfall estimates obtained through the bottom up
116 approach for hydrological and water resources applications have been recently published (e.g.,

117 [Ciabatta et al., 2016](#); [Abera et al., 2017](#); [Brunetti et al., 2018](#); [Camici et al., 2018](#)). These studies
118 have highlighted the large potential of this technique as a complimentary and useful approach
119 for estimating rainfall from space, and have also shown its main limitations. Specifically, the
120 temporal resolution and the accuracy of satellite soil moisture products play a fundamental role
121 in determining the accuracy of the bottom up rainfall estimates.

122 In this study, we describe the newly developed SM2RAIN-ASCAT rainfall data record
123 covering the period 2007-2018 and characterized by a spatial/temporal sampling of 12.5 km/1-
124 day. The new SM2RAIN-ASCAT data record is obtained from the application of SM2RAIN
125 algorithm ([Brocca et al., 2014](#)) to the ASCAT soil moisture data records H113 and H114
126 provided by the European Organisation for the Exploitation of Meteorological Satellites
127 (EUMETSAT) Satellite Application Facility on Support to Operational Hydrology and Water
128 Management (H SAF). It is the first SM2RAIN-ASCAT data record available at the same
129 spatial resolution as the ASCAT soil moisture product (previous data records have been under-
130 sampled at 0.5- and 1-degree resolution). Moreover, we have included the latest improvements
131 in pre- and post-processing of soil moisture and rainfall data as well as in the SM2RAIN
132 algorithm. The main differences with the SM2RAIN-CCI rainfall data record ([Ciabatta et al.,](#)
133 [2018](#)) are the input soil moisture product (the input of SM2RAIN-CCI is the European Space
134 Agency Climate Change Initiative Soil Moisture, ESA CCI soil moisture, product, [Dorigo et](#)
135 [al., 2017](#)), and the time coverage (SM2RAIN-CCI spans the period 1998-2015). Technically,
136 the use of the same satellite sensor in SM2RAIN-ASCAT data record is preferable to ensure
137 consistency between soil moisture estimates over time to which the SM2RAIN algorithm is
138 highly sensitive.

139 The purpose of this study is twofold. As a first objective, we have applied SM2RAIN
140 algorithm at 1009 points uniformly distributed (with spacing of 1.5°) in the United States, Italy,
141 India and Australia for testing different configurations of data pre-/post-processing and
142 SM2RAIN model equation. This analysis has allowed us to select the best configuration that is
143 implemented on a global scale for obtaining the SM2RAIN-ASCAT data record. The second
144 objective is the assessment of the global scale SM2RAIN-ASCAT data record through the
145 comparison with reference datasets and by exploiting the Triple Collocation (TC) approach
146 ([Massari et al., 2017a](#)). As reference datasets we have used high-quality local raingauge
147 networks from 2013 to 2017 in the United States, Italy, India and Australia for the assessment
148 at 1009 points and for the regional assessment. Three additional global datasets have been

149 considered: the latest reanalysis of the European Centre for Medium-Range Weather Forecasts
150 (ECMWF), ERA5, the gauge-based Global Precipitation Climatology Centre (GPCC), and the
151 GPM IMERG product (Early Run version). ERA5 has been used for the generation of the quasi-
152 global SM2RAIN-ASCAT data record; GPCC and GPM IMERG have been considered for the
153 TC analysis.

154 We underline that the paper goal is to present and describe the SM2RAIN-ASCAT quasi-
155 global rainfall data record and to perform a comparison with state-of-the-art global rainfall
156 products. We do not want to show a comprehensive assessment of the product. Indeed, we
157 believe that researchers other than the product developers should perform the validation of the
158 dataset. Even better, we stress the importance of performing the validation by using the datasets
159 in hydrological or agricultural applications (e.g., flood prediction and agricultural water
160 management).

161 **2 Datasets**

162 Nine different datasets have been collected for this study which are based on remote
163 sensing, ground observations and reanalysis. Refer to *Table 1* for a summary of the datasets.

164 The main input dataset for producing SM2RAIN-ASCAT data record is the ASCAT soil
165 moisture data record provided by the “EUMETSAT Satellite Application Facility on Support
166 to Operational Hydrology and Water Management (H SAF)” (<http://hsaf.meteoam.it/>).
167 ASCAT, currently on board Metop-A (launched on October 2006), Metop-B (September 2012)
168 and Metop-C (November 2018) satellites, is a scatterometer operating at C-band (5.255 GHz)
169 and, by using the TU Wien algorithm (Wagner et al., 2013) the H SAF provides a soil moisture
170 product characterized by 12.5 km spatial sampling. The temporal sampling is varying as a
171 function of latitude and the number of satellites: by using Metop-A only a daily sampling is
172 obtained, by using Metop-A and Metop-B two observations per day are available at mid-
173 latitudes. Here we have used the H SAF ASCAT soil moisture data record (using Metop-A and
174 Metop-B) available through the product H113 (PUM, 2018) covering the period 2007-2017 and
175 its extension product H114 for the year 2018.

176 Three datasets obtained from the latest reanalysis of ECMWF, i.e., ERA5, have been
177 used. ERA5 reanalysis is characterized by a spatial resolution of ~36 km and hourly temporal
178 resolution. ERA5 is available from the Copernicus Climate Change service and the datasets
179 cover the period 1979 to present. We have extracted hourly observations for the period 2007-

180 2018 for three variables: evaporation, soil temperature for the first layer (0-7 cm) and total
181 rainfall (computed as the difference between total precipitation and snowfall). Evaporation data
182 are used as additional input to the SM2RAIN algorithm and soil temperature data for masking
183 periods with frozen soils. Total rainfall has been considered as a benchmark for the calibration
184 of global SM2RAIN parameter values (see next section).

185 Ground-based rainfall datasets from regional networks have been also collected including
186 the Climate Prediction Center (CPC) Unified Gauge-Based Analysis of Daily Precipitation in
187 the United States, the gridded rainfall data provided by ~3000 stations of the National
188 Department of Civil Protection in Italy ([Ciabatta et al., 2017](#)), the India Meteorological
189 Department (IMD, http://www.imd.gov.in/pages/services_hydromet.php) rainfall observations
190 in India, and the Australia Water Availability Project (AWAP, <http://www.bom.gov.au/jsp/awap/rain/index.jsp>) gridded rainfall data in Australia. These
191 datasets have been used firstly for the selection of the optimal configuration of SM2RAIN
192 implementation. For that, 1009 points uniformly distributed over the four regions have been
193 selected. Secondly, the regional networks have been used for the assessment of the global
194 SM2RAIN-ASCAT rainfall product at regional scale.

196 The ERA5 and local rainfall datasets have been regridded over the ASCAT grid (12.5 km)
197 through the nearest neighbouring method and resampled at daily time scale as accumulated
198 rainfall from 00:00 to 23:59 UTC. The ERA5 evaporation and soil temperature data are also
199 regridded to the same grid and aggregated at daily scale as accumulated and average value from
200 00:00 to 23:59 UTC, respectively.

201 For the global assessment of SM2RAIN-ASCAT, two additional rainfall datasets have
202 been considered: Global Precipitation Climatology Centre (GPCC) Full Data Daily Product
203 ([Schamm et al., 2015](#)) and GPM IMERG Early Run product ([Hou et al., 2014](#)), hereinafter
204 referred to as GPM-ER. Due to the availability of GPM-ER from April 2014, the global analysis
205 has been carried out in the 4-year period from January 2014 to December 2018. Moreover, for
206 the global inter-comparison all the datasets (SM2RAIN-ASCAT, ERA5, GPCC, and IMERG-
207 ER) have been regridded at 0.25-degree resolution by spatially averaging the pixels contained
208 in each 0.25-degree cell for SM2RAIN-ASCAT and GPM-ER, and by selecting the nearest
209 pixel for ERA5 and GPCC.

210 **3 Methods**

211 In the following, the methodology used for obtaining the SM2RAIN-ASCAT data record
212 is described. Specifically, three steps are carried out (see *Figure 1*): 1) surface soil moisture
213 data pre-processing, 2) SM2RAIN algorithm, and 3) rainfall data post-processing. Different
214 configurations for the data pre-/post-processing and for the SM2RAIN model equation are
215 considered; the details are given in *Table 2*.

216 **3.1 Soil moisture data pre-processing**

217 The ASCAT surface soil moisture product is provided as relative soil moisture (between
218 0 and 1) at the overpass time of the satellite sensor (see *Figure A1* for the mean daily revisit
219 time of ASCAT in the period 2007-2012 with only Metop-A and the period 2013-2018 with
220 Metop-A+B). For the application of SM2RAIN algorithm, data should be equally spaced in
221 time and hence, we have linearly interpolated in time soil moisture observations every 24 hours,
222 12 hours and 8 hours. The interpolation may increase the risk of false rainfall events, but it is a
223 required step to obtain accumulated rainfall over a fixed duration. In a preliminary test (not
224 shown for brevity), we have tested the three sampling frequencies with the baseline formulation
225 for SM2RAIN (*equation 6*, see below). The best performances have been obtained with 12
226 hours sampling, particularly from 2013 to 2018 in which both Metop-A and -B are available.
227 Therefore, 12 hours sampling has been used in the following analyses. The 24-hour
228 accumulated rainfall is obtained by summing the two 12-hour accumulated rainfall data
229 obtained for each day.

230 One of the major problems in using satellite soil moisture observations for rainfall
231 estimation is related to the high frequency fluctuations caused by measurement and retrieval
232 errors. If positive, such fluctuations are interpreted erroneously as rainfall by SM2RAIN
233 algorithm. Therefore, satellite surface soil moisture data need to be filtered before being used
234 as input into SM2RAIN. In previous studies, the exponential filtering has been considered
235 (Wagner et al., 1999). The exponential filter, also known as Soil Water Index (SWI), has been
236 used for filtering surface soil moisture time series as a function of a single parameter, T , i.e.,
237 the characteristic time length. In this study, we have tested two additional filtering methods.
238 The first one is an extension of the exponential filter in which the T parameter is assumed to be
239 varying with soil moisture as proposed in Brocca et al. (2013b). Specifically, T decreases with
240 increasing soil moisture through a 2-parameter power law. Therefore, the data are filtered more

241 during dry conditions. The third approach that we have implemented is a discrete wavelet filter
242 (similar to [Massari et al., 2017b](#)). The discrete wavelet filter cuts the higher frequencies of the
243 signal, typically characterized by noises, over a threshold selected through the principle of
244 Stein's Unbiased Risk at multiple levels. We have found the Daubechies wavelets to be the most
245 appropriate functions because their shape and the shape of the soil moisture signal is similar.
246 Therefore, we have implemented a Daubechies-based wavelet filter in which the filtering level
247 is optimized.

248 For all the filtering approaches, the parameter values of the filters have been optimized
249 point-by-point in order to reproduce the reference rainfall observations.

250 **3.2 SM2RAIN algorithm and calibration**

251 The SM2RAIN algorithm is based on the inversion of the soil water balance equation and
252 allows to estimate the amount of water entering the soil by using as input soil moisture
253 observations from in situ or satellite sensors (e.g., [Brocca et al., 2013a; 2014; 2015](#); [Koster et al., 2016](#);
254 [Ciabatta et al., 2017](#); [Massari et al., 2014](#)). Specifically, the soil water balance
255 equation can be described by the following equation (over non-irrigated areas):

$$256 \quad nZ \frac{dS(t)}{dt} = p(t) - g(t) - sr(t) - e(t) \quad (1)$$

257 where n [-] is the soil porosity, Z [mm] is the soil layer depth, $S(t)$ [-] is the relative
258 saturation of the soil or relative soil moisture, t [days] is the time, $p(t)$ [mm/day] is the rainfall
259 rate, $g(t)$ [mm/day] is the drainage (deep percolation plus subsurface runoff) rate, $sr(t)$
260 [mm/day] is the surface runoff rate and $e(t)$ [mm/day] is the actual evapotranspiration rate.

261 For estimating the rainfall rate, *equation (1)* is applied only during rainfall periods and,
262 hence, some of the components of the equation can be considered as negligible. For instance,
263 the actual evapotranspiration rate during rainfall is quite low due to the presence of clouds and,
264 hence, the absence of solar radiation. Similarly, the surface runoff rate, i.e., the water that does
265 not infiltrate into the soil and flows at the surface to the watercourses, is much lower than the
266 rainfall rate, mainly if *equation (1)* is applied at coarse spatial resolution (20 km), i.e., with
267 satellite soil moisture data. Indeed, most of water becomes runoff flowing in the subsurface,
268 and also the part that does not infiltrate, due to for instance impervious land cover or soil, may
269 re-infiltrate downstream within a pixel at 20 km scale. We have indirectly tested this hypothesis
270 by counting the number of days the ASCAT soil moisture product is higher than 99.5 percentile

271 for two (or more) consecutive days in the period 2007-2018. We have indirectly tested this
 272 hypothesis by counting the number of days the ASCAT soil moisture product is higher than
 273 99.5 percentile for two (or more) consecutive days in the period 2007-2018. We have found
 274 that the number of consecutive days in which the soil is saturated is equal to 4 days (median
 275 value on a global scale) over 12 years, with 90% of land pixels with values lower than 12 days
 276 (i.e., 1 day per year). The occurrence of higher values is limited to very few areas in the tropical
 277 forests and over Himalaya (see **Figure A2**).

278 Following the indications obtained in [Brocca et al. \(2015\)](#), we have assumed the surface
 279 runoff rate, $sr(t)$, as negligible (i.e., Dunnian runoff) and we have rearranged **equation (1)** for
 280 estimating the rainfall rate:

$$281 \quad p(t) = nZ \frac{dS(t)}{dt} + g(t) + e(t) \quad (2)$$

282 In this study, we have considered different formulations for equation (2) by varying the
 283 drainage rate as:

$$284 \quad g(t) = K_s S(t)^m \quad (3.1)$$

$$285 \quad g(t) = K_s S(t)^{\lambda+1} \left[1 - \left(1 - S(t)^{\frac{\lambda+1}{\lambda}} \right)^{\frac{\lambda}{\lambda+1}} \right]^2 \quad (3.2)$$

$$286 \quad g(t) = K_s S(t)^\tau \left[1 - \left(1 - S(t)^{\frac{1}{m}} \right)^m \right]^2 \quad (3.3)$$

287 where K_s [mm/day] is the saturated hydraulic conductivity, m [-] and λ [-] are exponents related
 288 to the pore size distribution index, and τ is the tortuosity index. Specifically, the three equations
 289 represent the hydraulic conductivity - soil moisture formulation by Brooks-Corey (3.1), van
 290 Genuchten (3.2), and Mualem-van Genuchten (3.3).

291 The actual evapotranspiration rate has been considered as an additional input, together
 292 with soil moisture, here obtained from ECMWF reanalysis ERA5:

$$293 \quad e(t) = K_c ET_{ERA5}(t) \quad (4)$$

294 where $ET_{ERA5}(t)$ [mm/day] is the actual evapotranspiration rate obtained from ERA5 reanalysis
 295 and K_c [-] is a correction factor for taking into account potential bias in ERA5 estimates.

296 Moreover, we have considered an additional formulation in which Z is a function of soil
297 moisture taking into account the different penetration depth of satellite sensors as a function of
298 wetness conditions:

$$299 \quad Z = Z[0.1 + (1 - S(t)^c)] \quad (5)$$

300 where c exponent determines the rate of decrease of penetration depth with increasing soil
301 moisture.

302 Accordingly, we have used different formulations for equation (2) that are compared with
303 the baseline equation used in previous studies (e.g., [Brocca et al., 2014](#)):

$$304 \quad p(t) = Zn \frac{dS(t)}{dt} + K_s S(t)^m \quad (6)$$

305 In synthesis, we have investigated 3 different configurations (total of 5 options) for: 1)
306 selecting the best equation for the drainage rate (*equations 3*), 2) testing the possibility to
307 include the evapotranspiration component (*equation 4*), and 3) testing the use of a variable
308 penetration depth with soil moisture conditions (*equation 5*). Each new configuration has been
309 compared with the baseline (*equation 6*) in order to select the best configuration for SM2RAIN
310 algorithm (see *Figure 1*). For all configurations, negative rainfall values, that might occur
311 during some dry-down cycles, have been set equal to zero.

312 SM2RAIN parameter values are calibrated point-by-point by using the reference rainfall
313 as target. As objective function, we have used the minimization of the RMSE between
314 SM2RAIN-ASCAT and reference rainfall.

315 **3.3 Rainfall data post-processing**

316 The use of satellite soil moisture observations for obtaining rainfall estimates is affected
317 by errors in the input data and in the retrieval algorithm SM2RAIN. The correction of the
318 overall bias in the climatology is a simple and effective approach for mitigating part of such
319 errors. Specifically, we refer here to a static correction procedure that once calibrated for a time
320 period can be applied in the future periods, also for operational real time productions. We note
321 that a climatological correction is performed in several satellite rainfall datasets delivered in
322 near real-time (e.g., GPM-Early Run). We have implemented two different approaches for
323 climatological correction: 1) a cumulative density function (CDF) matching approach at daily
324 time scale, and 2) a monthly correction approach. Specifically, the implemented CDF matching
325 approach is a 5-order polynomial correction as described in [Brocca et al. \(2011\)](#) for matching

326 the CDF of estimated rainfall with respect to reference rainfall, in which the CDF are computed
327 over the whole calibration period at daily time scale. The monthly correction approach
328 computes the monthly ratios between the climatology of estimated and reference rainfall, i.e.,
329 12 correction factors per pixel. Then, the SM2RAIN-estimated rainfall is multiplied for the
330 monthly correction factors to obtain the climatologically corrected SM2RAIN-estimated
331 rainfall.

332 **3.4 Triple collocation analysis**

333 For the global assessment of satellite, reanalysis and gauge-based rainfall products we
334 have used the Triple Collocation (TC) technique. TC can theoretically provide error and
335 correlations of three products (a triplet) given that each of the three products is afflicted by
336 mutually independent errors. Therefore, in principle, TC can be used for assessing the quality
337 of satellite products without using ground observations ([Massari et al., 2017a](#)). In this study,
338 we have implemented the same procedure as described in [Massari et al. \(2017\)](#), i.e., by
339 implementing an additive error model at daily time scale, and we refer the reader to this study
340 for the analytical details. In synthesis, by using the extended TC method firstly proposed by
341 [McColl et al. \(2014\)](#), it is possible to estimate the temporal correlation, R_{TC} , of each rainfall
342 product in the triplets with the truth.

343 **3.5 Performance scores**

344 Several metrics have been used to assess the product performance during the validation
345 period. As continuous scores we have computed the Pearson's correlation coefficient (R), the
346 root mean square error (RMSE), the mean error between estimated and reference rainfall
347 (BIAS), and the ratio of temporal variability of estimated and reference rainfall (STDRATIO).
348 Continuous scores have been computed on a pixel-by-pixel basis by considering 1 day of
349 accumulated rainfall. Moreover, three categorical scores, i.e. Probability of Detection (POD),
350 False Alarm Ration (FAR) and Threat Score (TS), have been computed. POD is the fraction of
351 correctly identified rainfall events (optimal value $POD=1$), FAR is the fraction of predicted
352 events that are non-events (optimal value $FAR=0$), while TS provides a combination of the
353 other two scores (optimal value $TS=1$). The categorical assessment is carried out by considering
354 a rainfall threshold of 0.5 mm/day (instead of 0 mm/day) in order to exclude spurious events
355 that might be due to rainfall interpolation\regridding in the reference datasets. For a complete
356 description of the performance scores, see *Table A1* in the Appendix.

357 4 Results

358 The results are split in three parts: 1) selection of the optimal configuration of SM2RAIN
359 through the assessment at 1009 points, 2) generation of global SM2RAIN-ASCAT rainfall data
360 record, and 3) regional assessment of SM2RAIN-ASCAT with gauge-based rainfall datasets
361 and global assessment through TC.

362 4.1 Selection of the best SM2RAIN processing configuration at 1009 points

363 As a first step we have co-located satellite soil moisture data from ASCAT soil moisture
364 H113+H114, ground-based rainfall observations and actual evapotranspiration data from ERA5
365 in space and time at 1009 points. We have selected 1009 points uniformly distributed over a
366 regular grid with spacing of 1.5° . Each point is considered representative of a $0.25^\circ \times 0.25^\circ$
367 box. The selection is carried out for reducing the computational time in running the different
368 SM2RAIN configurations. The numbers of points for each region is depending on the size of
369 the region: 328 points in Australia, 163 in India, 55 in Italy, and 463 in the United States.
370 Ground observations, GPM-ER and ERA5 data are regridded by spatial averaging
371 measurements contained over each $0.25^\circ \times 0.25^\circ$ box. These datasets are made freely available
372 here (<https://doi.org/10.5281/zenodo.2580285>, Brocca, 2019) for those interested to test
373 alternative approaches for rainfall estimation from ASCAT soil moisture. Specifically, we have
374 considered the period 2013-2016, 2013-2014 for the calibration and 2015-2016 for the
375 validation; in the sequel only the results in the validation period are shown. The ground-based
376 high quality rainfall observations available for the four regions are used as reference data
377 (ground truth) in this analysis. The reference configuration, REF, as used in previous SM2RAIN
378 applications (e.g., Brocca et al., 2014), uses the SWI for data filtering, the SM2RAIN
379 formulation as in *equation (6)*, and no climatological correction. Results in the validation period
380 are shown in *Figure 2A* in terms of temporal R against reference data. As shown, the median
381 R for all points is equal to 0.60, with better results in Italy (median R=0.67, see boxplots) and
382 similar results in the other 3 regions (median R=0.60 and 0.59). These results are in line with
383 previous studies (e.g., Ciabatta et al., 2017; Tarpanelli et al., 2017) carried out in Italy and India
384 and highlight the potential of ASCAT soil moisture observations to provide daily rainfall
385 estimates. *Figure 3* (first column) shows the results for the different performance metrics; in
386 the last two columns the results obtained with GPM-ER and ERA5 are shown for comparison.
387 Very good statistics have been obtained in terms of RMSE and BIAS but a tendency to
388 underestimate the observed rainfall variability (median STD RATIO=0.60) and medium-high

389 probability of false alarm (median FAR=0.53). The other scores are similar, or slightly lower
390 than those obtained through GPM-ER and ERA5.

391 The first test has been dedicated to the filtering of soil moisture data by using three
392 approaches: 1) SWI, i.e., the REF configuration, 2) SWI with T varying with soil moisture,
393 SWI-Tvar, and 3) the discrete wavelet filtering, WAV. **Figure 3** shows in the first three columns
394 the summary of the performance scores highlighting that the SWI-Tvar configuration is
395 performing the best, even though the differences with REF configuration are small. **Figure 2b**
396 shows the R map for SWI-Tvar configuration while in **Figure 2c** the differences in R-values
397 with REF are displayed. Improved performance in terms of R is visible over most of the pixels
398 except in central Australia.

399 The second test has been performed on the SM2RAIN equation by using different
400 drainage functions (VGEN and MUA configurations), by adding the evapotranspiration
401 component (EVAP), and by considering the variability of sensing depth, Z, with soil moisture
402 (ZVAR). VGEN, MUA and ZVAR configurations are characterized by lower performances
403 than REF (see **Figure 3**, columns 4, 5 and 7), even though MUA and ZVAR incorporate an
404 additional parameter to be calibrated (and, hence, better performance was expected). The
405 addition of evapotranspiration brings a slight improvement with respect to REF (see **Figure 3**,
406 column 6), with results similar to SWI-Tvar. Larger improvements are obtained over areas in
407 which evapotranspiration is more important, e.g., in the south-western United States and central
408 western Australia. In India and Italy, the results are very similar to REF. However, EVAP
409 configuration requires actual evapotranspiration data from ERA5 as additional input and such
410 data might be not available for the implementation of the processing algorithm in an operational
411 context.

412 The final test has been done by applying the daily CDF matching, BC-CDF, and monthly
413 correction factors, BC-MON, for correcting the climatological bias in SM2RAIN-derived
414 rainfall estimates; results are shown in columns 8 and 9 of **Figure 3**. For these two
415 configurations, the improvements with respect to REF are evident but with different magnitude
416 for the different scores. BC-CDF improves significantly STDRATIO, TS and FAR with a slight
417 deterioration in R and RMSE. BC-MON shows the highest R-values among all configurations
418 with the larger improvements in India, Italy and United States. However, the improvement in
419 terms of STDRATIO, TS and FAR is less important than BC-CDF. Therefore, depending on
420 which score is assumed more important, one of the two configurations can be selected. If

421 compared with GPM-ER, BC-CDF and BC-MON configurations show similar results with
422 larger positive differences, in terms of RMSE, BIAS, STDRATIO and POD; R values are
423 slightly better for GPM-ER that is also much better in terms of TS and FAR. Similar findings
424 can be summarized in the comparison with ERA5, even though ERA5 is performing the best in
425 terms of R, STDRATIO, FAR, and TS among all configurations.

426 *Figure 4* shows time series of rainfall averaged over the four regions as obtained from
427 ground observations and from BC-MON configuration. The agreement of spatially averaged
428 rainfall with observations is high with R-values greater than 0.83, and very low BIAS.
429 Moreover, regional scale rainfall events are correctly reproduced both in terms of timing and
430 magnitude.

431 **4.2 Generation of SM2RAIN-ASCAT data record**

432 Based on the tests performed in the previous paragraph, we have selected the best
433 configuration using SWI-Tvar for filtering, Brooks-Corey function for losses, and the monthly
434 correction approach for climatological correction. The addition of evapotranspiration
435 component, even though showing some improvements, has been not used in view of an
436 operational implementation of the method. The monthly correction approach has been selected
437 as R and RMSE scores have been considered more important based on previous investigations
438 on the assessment of satellite rainfall products (e.g., [Massari et al., 2017](#)).

439 The selected configuration has been applied on a global scale to 839826 points over which
440 ASCAT soil moisture observations are available. As reference dataset for the calibration of the
441 parameter values of the pre-processing (filtering), of SM2RAIN, and of the post-processing,
442 the ERA5 rainfall has been used mainly because of its higher spatial resolution compared to
443 GPCP (36 km versus 100 km). However, we have also tested the use of the two datasets for
444 calibration at randomly chosen 20000 points which showed that the estimated rainfall in the
445 two calibration tests is very similar. For instance, the median R between the two SM2RAIN-
446 ASCAT data records is higher than 0.90 (not shown for brevity). This result clearly demonstrate
447 that the selection of reference dataset has a small influence on SM2RAIN-derived rainfall that
448 is mostly driven from soil moisture temporal fluctuations. Additionally, considering the
449 improved ASCAT coverage after 2013, the calibration has been split from 2007 to 2012
450 (Metop-A) and from 2013 to 2018 (Metop-A and -B). The dual calibration has solved the issue
451 in terms of long-term trend that has been found in previous application of SM2RAIN to ASCAT

452 soil moisture data (Beck et al., 2017). Finally, we have flagged rainfall observations in space
453 and time when the data are supposed to be less reliable. In space (i.e., a fixed spatial mask), we
454 have used the committed area mask developed for the ASCAT soil moisture product (i.e., the
455 area in which the ASCAT soil moisture retrievals are expected to be good, PVR 2017), a frozen
456 probability mask and a topographic complexity mask. In time (i.e., a temporally variable mask),
457 we have considered the soil temperature data from ERA5 and flagged the observations with soil
458 temperature values between 0°C and 3°C as temporary frozen soil and below 3°C as frozen soil.
459 As many applications require continuous data, we have preferred to flag the data instead of
460 removing them with an expected loss of accuracy.

461 The SM2RAIN-ASCAT data record so obtained has a spatial sampling of 12.5 km, a daily
462 temporal resolution and covers the 12-year period 2007-2018. **Figure 5** shows R and RMSE
463 values between SM2RAIN-ASCAT and ERA5 in a single map. Therefore, **Figure 5** illustrates
464 the consistency between SM2RAIN-ASCAT and ERA5, and it is not intended to assess the
465 performance of the data record (even though we expect better accuracy in areas where the
466 agreement is higher). Green light colours indicate very good agreement with high R and low
467 RMSE, orange to red colours indicate low R and high RMSE, while black colour indicates low
468 RMSE and R highlighting areas in which rainfall occurrence and variability is very low (e.g.,
469 Sahara Desert, high latitudes). The data record has been found in very good agreement with
470 ERA5 (high R and low RMSE) in western United States, Brazil, southern and western South
471 America, southern Africa, Sahel, southern-central Eurasia, and Australia. The areas in which
472 SM2RAIN-ASCAT is characterized by lower consistency with ERA5 are those with dense
473 vegetation (Amazon, Congo, and Indonesia), with complex topography (e.g., Alps, Himalaya,
474 Andes), at high latitudes and Saharan and Arabian deserts. In these areas it is well-known that
475 the ASCAT soil moisture product has limitations (e.g., Wagner et al., 2013), and generally the
476 retrieval of soil moisture from remote sensing is more challenging. The median R and RMSE
477 values are equal to 0.56 and 3.06 mm/day, with slightly better scores in the period 2013-2018
478 (R=0.57, RMSE=2.95), thanks to the availability of ASCAT on both Metop-A and Metop-B.

479 **4.3 Regional and global assessment of SM2RAIN-ASCAT data record**

480 By using all the pixels included in the four regions (Italy, United States, India and
481 Australia), for a total of 29843 points, the new SM2RAIN-ASCAT rainfall data record has been
482 compared with reference rainfall observations in **Figure 6**, by considering the whole period
483 2007-2018. Specifically, the box plots of different performance metrics (the same of **Figure 3**)

484 are shown and compared with the results obtained through GPCC, ERA5, and GPM-ER. By
485 focusing on the SM2RAIN-ASCAT data record performance over the different regions, it
486 shows better performance in Italy (median $R=0.67$) and United States (median $R=0.62$), almost
487 comparable with the other datasets; while in Australia and India R -values are lower (median
488 $R=0.61$ and 0.59). In the selected regions, the best product is GPCC (mainly in Australia)
489 followed by ERA5 while GPM-ER and SM2RAIN-ASCAT are performing similarly in terms
490 of R . The better performance of GPCC are expected (gauge-based dataset) and also the very
491 good performance of ERA5 in Italy and Australia thanks to the availability of ground
492 observations for the reanalysis. We highlight also that differently from SM2RAIN-ASCAT and
493 GPM-ER, GPCC and ERA5 have a latency of weeks to months and, hence, these products
494 cannot be used for near real time applications. When considering the RMSE score, the results
495 are quite different with respect to R . SM2RAIN-ASCAT is overall very good being the best
496 (second best) product in United States (India). The ranking of the product is GPCC, SM2RAIN-
497 ASCAT, ERA5 and GPM-ER, with the latter showing high RMSE values in United States and
498 Australia. As obtained in previous studies ([Brocca et al., 2016](#); [Ciabatta et al., 2017](#)), the
499 SM2RAIN approach is very good in obtaining low RMSE values thanks to its accuracy in the
500 retrieval of accumulated rainfall. Moreover, the product accuracy is stable over time as it is not
501 as strongly affected by the availability of satellite overpasses as in the top down approach. As
502 shown also in **Figure 3**, the SM2RAIN-ASCAT data record has limitations in reproducing the
503 variability of rainfall (low STDRATIO) mainly due underestimation issues. Moreover, FAR
504 values of SM2RAIN-ASCAT are quite high highlighting the difficulties in removing the
505 problem of high frequency soil moisture fluctuations wrongly interpreted by SM2RAIN as
506 rainfall events.

507 On a global scale, the TC approach has been implemented by using the triplet SM2RAIN-
508 ASCAT, GPM-ER and GPCC, by considering the common period 2015-2018 and at daily time
509 scale. In TC analysis we have not considered ERA5 purposely to avoid any dependency
510 between the products. Theoretically, the extended TC approach provides the correlation, R_{TC} ,
511 against the underlying “truth”. **Figures 7A and 7B** show the R_{TC} maps for SM2RAIN-ASCAT
512 and GPM-ER highlighting similar mean values (0.66 and 0.64 for SM2RAIN-ASCAT and
513 GPM-ER, respectively). It should be underlined that the R_{TC} values are higher than those
514 obtained in the comparison with ground observations as theoretically the metric does not
515 contain the error in the reference ([Massari et al., 2017a](#)). The spatial pattern of the performance
516 is quite different as demonstrated in **Figure 7c** in which the differences between the two R_{TC}

517 maps is shown. Again, these results underline the strong complementarity between bottom up
518 and top down approaches (e.g., [Ciabatta et al., 2017](#); [Chiaravallotti et al., 2018](#)). As expected,
519 SM2RAIN-ASCAT performs worse over desert areas, tropical forests and complex
520 mountainous regions. Differently, over plains and low vegetated areas SM2RAIN-ASCAT is
521 performing better than GPM-ER, particularly in the southern hemisphere. Indeed, in Africa and
522 South America SM2RAIN-ASCAT provides good performance (see also [Figure 7A](#)) thanks to
523 the capability of the bottom up approach to estimate accumulated rainfall accurately with a
524 limited number of satellite overpasses occurring in these areas, differently from the top down
525 approach used in GPM-ER.

526 The box plots of R_{TC} shown in [Figure 7D](#) indicates that, overall, GPCC is performing
527 similar to the two satellite products with major differences in the spatial patterns of the
528 performance. SM2RAIN-ASCAT is performing the best among the three products in Africa,
529 South America, central-western United States and central Asia while GPCC is performing the
530 best in the remaining parts except the tropical region in which GPM-ER is performing very
531 good (see [Figure 8](#)). If we consider only the committed area of ASCAT ([PVR 2017](#)), in which
532 the soil moisture product is supposed to be reliable, the mean value of R_{TC} is equal to 0.72
533 whereas in the masked area it is equal to 0.59.

534 **5 Data availability**

535 The SM2RAIN-ASCAT data record is freely available at
536 <https://doi.org/10.5281/zenodo.2591215> ([Brocca et al., 2019](#)).

537 **6 Conclusions**

538 In this study, we have described the development of a new SM2RAIN-ASCAT rainfall
539 data record highlighting the steps carried out for improving the retrieval algorithm and the pre-
540 /post-processing of the data. The major novelties of the SM2RAIN-ASCAT rainfall data record
541 developed here with respect to previous versions are: 1) application of SM2RAIN at full spatial
542 resolution thus providing a gridded data record with sampling of 12.5 km, 2) improved sampling
543 and filtering of ASCAT soil moisture data, 3) application of monthly climatological correction,
544 and 4) improved calibration strategy.

545 The SM2RAIN-ASCAT data record has been preliminary assessed at regional ([Figures](#)
546 [4 and 6](#)) and global ([Figure 5, 7 and 8](#)) scale in terms of different performance metrics with

547 larger emphasis on the temporal correlation, R, and the root mean square error, RMSE. The
548 overall performances are good, mainly in terms of RMSE thanks to the capacity of SM2RAIN
549 to accurately reproduce accumulated rainfall consistently over time. Importantly, SM2RAIN-
550 ASCAT is found to perform even better than ground-based GPCP product over the southern
551 hemisphere in Africa and South America, and in central-western United States and central Asia.
552 Limitations of SM2RAIN-ASCAT data record consist in: 1) the underestimation of peak
553 rainfall events, 2) the presence of spurious rainfall events due to high frequency soil moisture
554 fluctuations, 3) the estimation of liquid rainfall only (snowfall cannot be estimated), and 4) the
555 possibility to estimate rainfall over land only.

556 In the near future, we are going to develop the near real-time version of the SM2RAIN-
557 ASCAT rainfall product that can be used as input for applications such as flood prediction
558 (similarly to [Camici et al., 2018](#) and [Massari et al., 2018](#)), landslide prediction ([Brunetti et al.,](#)
559 [2018](#)) and novel applications for the agriculture and for the water resources management.

560

561 **Acknowledgments:** The authors gratefully acknowledge support from the EUMETSAT
562 through the Global SM2RAIN project (contract n° EUM/CO/17/4600001981/BBo) and the
563 “Satellite Application Facility on Support to Operational Hydrology and Water Management
564 (H SAF)” CDOP 3 (EUM/C/85/16/DOC/15).

- 566 Abera, W., Formetta, G., Brocca, L., Rigon, R.: Modeling the water budget of the Upper Blue
567 Nile basin using the JGrass-NewAge model system and satellite data. *Hydrology and*
568 *Earth System Sciences*, 21, 3145-3165, 2017.
- 569 Beck, H.E., Vergopolan, N., Pan, M., Levizzani, V., van Dijk, A.I.J.M., Weedon, G., Brocca,
570 L., Pappenberger, F., Huffman, G.J., Wood, E.F. (2017). Global-scale evaluation of 22
571 precipitation datasets using gauge observations and hydrological modeling. *Hydrology*
572 *and Earth System Sciences*, 21, 6201-6217.
- 573 Brocca, L., Hasenauer, S., Lacava, T., Melone, F., Moramarco, T., Wagner, W., Dorigo, W.,
574 Matgen, P., Martínez-Fernández, J., Llorens, P., Latron, J., Martin, C., Bittelli, M.: Soil
575 moisture estimation through ASCAT and AMSR-E sensors: an intercomparison and
576 validation study across Europe. *Remote Sensing of Environment*, 115, 3390-3408, 2011.
- 577 Brocca, L., Melone, F., Moramarco, T., Wagner, W.: A new method for rainfall estimation
578 through soil moisture observations. *Geophysical Research Letters*, 40(5), 853-858,
579 2013a.
- 580 Brocca, L., Melone, F., Moramarco, T., Wagner, W., Albergel, C.: Scaling and filtering
581 approaches for the use of satellite soil moisture observations. In: George P. Petropoulos
582 (ed.), *Remote Sensing of Energy Fluxes and Soil Moisture Content*, CRC Press 2013,
583 Chapter 17, 411-426, ISBN: 978-1-4665-0578-0, 2013b.
- 584 Brocca, L., Ciabatta, L., Massari, C., Moramarco, T., Hahn, S., Hasenauer, S., Kidd, R., Dorigo,
585 W., Wagner, W., Levizzani, V.: Soil as a natural rain gauge: estimating global rainfall
586 from satellite soil moisture data. *Journal of Geophysical Research*, 119(9), 5128-5141,
587 2014, 2014.
- 588 Brocca, L., Massari, C., Ciabatta, L., Moramarco, T., Penna, D., Zuecco, G., Pianezzola, L.,
589 Borga, M., Matgen, P., Martínez-Fernández, J.: Rainfall estimation from in situ soil
590 moisture observations at several sites in Europe: an evaluation of SM2RAIN algorithm.
591 *Journal of Hydrology and Hydromechanics*, 63(3), 201-209, 2015.
- 592 Brocca, L., Pellarin, T., Crow, W.T., Ciabatta, L., Massari, C., Ryu, D., Su, C.-H., Rudiger, C.,
593 Kerr, Y.: Rainfall estimation by inverting SMOS soil moisture estimates: a comparison
594 of different methods over Australia. *Journal of Geophysical Research*, 121(20), 12062-
595 12079, 2016.
- 596 Brocca, L., Crow, W.T., Ciabatta, L., Massari, C., de Rosnay, P., Enenkel, M., Hahn, S.,
597 Amarnath, G., Camici, S., Tarpanelli, A., Wagner, W.: A review of the applications of
598 ASCAT soil moisture products. *IEEE Journal of Selected Topics in Applied Earth*
599 *Observations and Remote Sensing*, 10(5), 2285-2306, 2017.
- 600 Brocca, L.: SM2RAIN test dataset with ASCAT satellite soil moisture (Version 1.0) [Data set].
601 Zenodo. <https://doi.org/10.5281/zenodo.2580285>, 2019.
- 602 Brocca, L., Filippucci, P., Hahn, S., Ciabatta, L., Massari, C., Camici, S., Schüller, L., Bojkov,
603 B., Wagner, W.: SM2RAIN-ASCAT (2007-2018): global daily satellite rainfall from
604 ASCAT soil moisture (Version 1.0) [Data set]. Zenodo.
605 <https://doi.org/10.5281/zenodo.2591215>, 2019.
- 606 Brunetti, M.T., Melillo, M., Peruccacci, S., Ciabatta, L., Brocca, L.: How far are we from the
607 use of satellite data in landslide forecasting? *Remote Sensing of Environment*, 210, 65-
608 75, doi:10.1016/j.rse.2018.03.016, 2018.

- 609 Camici, S., Ciabatta, L., Massari, C., Brocca, L.: How reliable are satellite precipitation
610 estimates for driving hydrological models: a verification study over the Mediterranean
611 area. *Journal of Hydrology*, 563, 950-961, 2018.
- 612 Chiaravalloti, F., Brocca, L., Procopio, A., Massari, C., Gabriele, S.: Assessment of GPM and
613 SM2RAIN-ASCAT rainfall products over complex terrain in southern Italy. *Atmospheric
614 Research*, 206, 64-74, 2018.
- 615 Ciabatta, L., Brocca, L., Massari, C., Moramarco, T., Gabellani, S., Puca, S., Wagner, W.:
616 Rainfall-runoff modelling by using SM2RAIN-derived and state-of-the-art satellite
617 rainfall products over Italy. *International Journal of Applied Earth Observation and
618 Geoinformation*, 48, 163-173, 2016.
- 619 Ciabatta, L., Marra, A.C., Panegrossi, G., Casella, D., Sanò, P., Dietrich, S., Massari, C.,
620 Brocca, L.: Daily precipitation estimation through different microwave sensors:
621 verification study over Italy. *Journal of Hydrology*, 545, 436-450, 2017.
- 622 Ciabatta, L., Massari, C., Brocca, L., Gruber, A., Reimer, C., Hahn, S., Paulik, C., Dorigo, W.,
623 Kidd, R., Wagner, W.: SM2RAIN-CCI: a new global long-term rainfall data set derived
624 from ESA CCI soil moisture. *Earth System Science Data*, 10, 267-280, 2018.
- 625 Crow, W.T., Huffman, G.F., Bindlish, R., Jackson, T.J.: Improving satellite rainfall
626 accumulation estimates using spaceborne soil moisture retrievals. *Journal of
627 Hydrometeorology*, 10, 199-212, 2009.
- 628 Crow, W.T., van den Berg, M.J., Huffman, G.J., Pellarin, T.: Correcting rainfall using satellite-
629 based surface soil moisture retrievals: The Soil Moisture Analysis Rainfall Tool
630 (SMART). *Water Resources Research*, 47, W08521, 2011.
- 631 Dorigo, W., Wagner, W., Albergel, C., Albrecht, F., Balsamo, G., Brocca, L., Chung, D., Ertl,
632 M., Forkel, M., Gruber, A., Haas, D., Hamer, P., Hirschi, M., Ikonen, J., de Jeu, R., Kidd,
633 R., Lahoz, W., Liu, Y.Y., Miralles, D., Mistelbauer, T., Nicolai-Shaw, N., Parinussa, R.,
634 Pratola, C., Reimer, C., van der Schalie, R., Seneviratne, S.I., Smolander, T., Lecomte,
635 P.: ESA CCI soil moisture for improved earth system understanding: state-of-the art and
636 future directions. *Remote Sensing of Environment*, 203, 185-215, 2017.
- 637 Ebert, E.E., Janowiak, J.E., Kidd, C.: Comparison of near-real-time precipitation estimates from
638 satellite observations and numerical models. *Bulletin of the American Meteorological
639 Society*, 88(1), 47-64, 2007.
- 640 Forootan, E., Khaki, M., Schumacher, M., Wulfmeyer, V., Mehrnegar, N., van Dijk, A.I.J.M.,
641 Brocca, L., Farzaneh, S., Akinluyi, F., Ramillien, G., Shum, C.K., Awange, J., Mostafaie,
642 A.: Understanding the global hydrological droughts of 2003-2016 and their relationships
643 with teleconnections. *Science of the Total Environment*, 650, 2587-2604, 2019.
- 644 Herold, N., Alexander, L.V., Donat, M.G., Contractor, S., Becker, A.: How much does it rain
645 over land? *Geophysical Research Letters*, 43(1), 341-348, 2016.
- 646 Hou, A.Y., Kakar, R.K., Neeck, S., Azarbarzin, A.A., Kummerow, C.D., Kojima, M., Oki, R.,
647 Nakamura, K., Iguchi, T.: The Global Precipitation Measurement (GPM) mission.
648 *Bulletin of the American Meteorological Society*, 95(5), 701-722, 2014.
- 649 Kidd, C., Levizzani, V.: Status of satellite precipitation retrievals. *Hydrology and Earth System
650 Sciences*, 15, 1109-1116, 2011.

- 651 Kidd, C., Becker, A., Huffman, G. J., Muller, C. L., Joe, P., Skofronick-Jackson, G.,
652 Kirschbaum, D. B.: So, how much of the Earth's surface is covered by rain gauges?
653 *Bulletin of the American Meteorological Society*, 98(1), 69-78, 2017.
- 654 Kirschbaum, D., Stanley, T.: Satellite-Based Assessment of Rainfall-Triggered Landslide
655 Hazard for Situational Awareness. *Earth's Future*, 6(3), 505-523, 2018.
- 656 Koster, R.D., Brocca, L., Crow, W.T., Burgin, M.S., De Lannoy, G.J.M.: Precipitation
657 Estimation Using L-Band and C-Band Soil Moisture Retrievals. *Water Resources*
658 *Research*, 52(9), 7213-7225, 2016.
- 659 Lanza, L.G., Vuerich, E.: The WMO Field Intercomparison of Rain Intensity Gauges.
660 *Atmospheric Research*, 94, 534-543, 2009.
- 661 Maggioni, V., Massari, C.: On the performance of satellite precipitation products in riverine
662 flood modeling: A review. *Journal of Hydrology*, 558, 214-224, 2018.
- 663 Massari, C., Brocca, L., Moramarco, T., Tramblay, Y., Didon Lescot, J.-F.: Potential of soil
664 moisture observations in flood modelling: estimating initial conditions and correcting
665 rainfall. *Advances in Water Resources*, 74, 44-53, 2014.
- 666 Massari, C., Crow, W., Brocca, L.: An assessment of the accuracy of global rainfall estimates
667 without ground-based observations. *Hydrology and Earth System Sciences*, 21, 4347-
668 4361, 2017a.
- 669 Massari, C., Su, C.-H., Brocca, L., Sang, Y.F., Ciabatta, L., Ryu, D., Wagner, W.: Near real
670 time de-noising of satellite-based soil moisture retrievals: An intercomparison among
671 three different techniques. *Remote Sensing of Environment*, 198, 17-29, 2017b.
- 672 Massari, C., Maggioni, V., Barbetta, S., Brocca, L., Ciabatta, L., Camici, S., Moramarco, T.,
673 Coccia, G., Todini, E.: Complementing near-real time satellite rainfall products with
674 satellite soil moisture-derived rainfall through a Bayesian inversion approach. *Journal of*
675 *Hydrology*, in press, 2019.
- 676 McColl, K.A., Vogelzang, J., Konings, A.G., Entekhabi, D., Piles, M., Stoffelen, A.: Extended
677 triple collocation: estimating errors and correlation coefficients with respect to an
678 unknown target. *Geophys. Res. Lett.*, 41, 6229-6236, 2014.
- 679 Overeem, A., Leijnse, H., Uijlenhoet, R.: Measuring urban rainfall using microwave links from
680 commercial cellular communication networks. *Water Resources Research*, 47(12),
681 doi:10.1029/2010WR010350, 2011.
- 682 Pellarin, T., Louvet, S., Gruhier, C., Quantin, G., Legout, C.: A simple and effective method
683 for correcting soil moisture and precipitation estimates using AMSR-E measurements.
684 *Remote Sensing of Environment*, 136, 28-36, 2013.
- 685 Pendergrass, A.G., Knutti, R.: The uneven nature of daily precipitation and its change.
686 *Geophysical Research Letters*, 45(21), 11980-11988, 2018.
- 687 "Product User Manual (PUM) Soil Moisture Data Records, Metop ASCAT Soil Moisture Time
688 Series": Tech. Rep. Doc. No: SAF/HSAF/CDOP3/PUM, version 0.7, 2018.
- 689 "Product Validation Report (PVR) Metop ASCAT Soil Moisture CDR products": Tech. Rep.
690 Doc. No: SAF/HSAF/CDOP3/PVR, version 0.6, 2017.

- 691 Rinaldo, A., Bertuzzo, E., Mari, L., Righetto, L., Blokesch, M., Gatto, M., Casagrandi, R.,
692 Murray, M., Vesenbeckh, S.M., Rodriguez-Iturbe, I.: Reassessment of the 2010–2011
693 Haiti cholera outbreak and rainfall-driven multiseason projections. *Proceedings of the*
694 *National Academy of Sciences*, 109(17), 6602-6607, 2012.
- 695 Román-Cascón, C., Pellarin, T., Gibon, F., Brocca, L., Cosme, E., Crow, W., Fernández, D.,
696 Kerr, Y., Massari, C.: Correcting satellite-based precipitation products through SMOS
697 soil moisture data assimilation in two land-surface models of different complexity: API
698 and SURFEX. *Remote Sensing of Environment*, 200, 295-310, 2017.
- 699 Schamm, K., Ziese, M., Raykova, K., Becker, A., Finger, P., Meyer-Christoffer, A., Schneider,
700 U.: GPCP Full Data Daily Version 1.0 at 1.0°: Daily Land-Surface Precipitation from
701 Rain-Gauges built on GTS-based and Historic Data.
702 doi:10.5676/DWD_GPCP/FD_D_V1_100, 2015.
- 703 Tarpanelli, A., Massari, C., Ciabatta, L., Filippucci, P., Amarnath, G., Brocca, L.: Exploiting a
704 constellation of satellite soil moisture sensors for accurate rainfall estimation. *Advances*
705 *in Water Resources*, 108, 249-255, 2017.
- 706 Thaler, S., Brocca, L., Ciabatta, L., Eitzinger, J., Hahn, S., Wagner, W.: Effects of different
707 spatial precipitation input data on crop model outputs under a Central European climate.
708 *Atmosphere*, 9(8), 290, 2018.
- 709 Trenberth, K.E., Asrar, G.R.: Challenges and opportunities in water cycle research: WCRP
710 contributions. *Surv. Geophys.* 35(3), 515-532, 2014.
- 711 Wagner, W., Lemoine, G. Rott, H.: A method for estimating soil moisture from ERS
712 scatterometer and soil data. *Remote Sens. Environ.*, 70, 191-207, 1999.
- 713 Wagner, W., Hahn, S., Kidd, R., Melzer, T., Bartalis, Z., Hasenauer, S., Figa, J., de Ros-
714 nay, P., Jann, A., Schneider, S., Komma, J., Kubu, G., Brugger, K., Aubrecht, C., Zuger, J.,
715 Gangkofner, U., Kienberger, S., Brocca, L., Wang, Y., Bloeschl, G., Eitzinger, J.,
716 Steinnocher, K., Zeil, P., Rubel, F.: The ASCAT soil mois- ture product: a review of its
717 specifications, validation results, and emerging applications. *Meteorologische Zeitschrift*
718 22 (1), 5-33, 2013.
- 719 Wanders, N., Pan, M., Wood, E.F.: Correction of real-time satellite precipitation with multi-
720 sensor satellite observations of land surface variables. *Remote Sensing of Environment*,
721 160, 206-221, 2015.
- 722 Wang, Z., Zhong, R., Lai, C., Chen, J.: Evaluation of the GPM IMERG satellite-based
723 precipitation products and the hydrological utility. *Atmospheric research*, 196, 151-163,
724 2017.
- 725 Zhang, Z., Wang, D., Wang, G., Qiu, J., Liao, W.: Use of SMAP soil moisture and fitting
726 methods in improving GPM estimation in near real time. *Remote Sensing*, 11, 368, 2019.

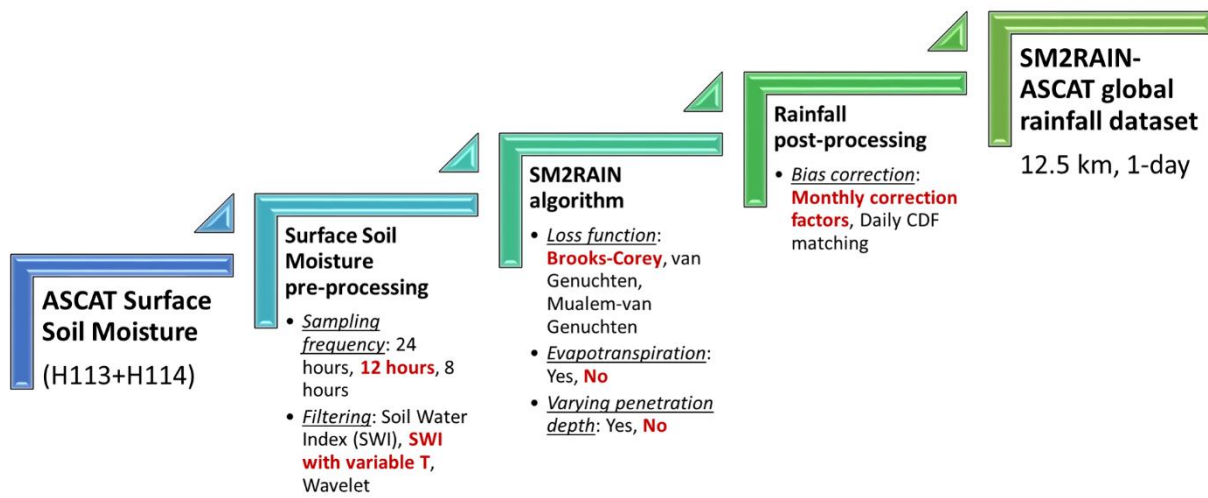
728 **Table 1.** List of satellite, ground-based and reanalysis products used in this study (the
729 spatial/temporal sampling used in this study is reported).

Short name	Full name and details	Data source	Spatial/temporal sampling	Time period	References
SOIL MOISTURE					
ASCAT	Advanced Scatterometer	satellite	12.5 km/daily	2007 - present	<u>Wagner et al. (2013)</u>
RAINFALL					
ERA5	ECMWF	reanalysis	0.25°/daily	1979 - present	<u>https://cds.climate.copernicus.eu/cdsapp#!/dataset/reanalysis-era5-single-levels?tab=overview</u>
GPCC	Global Precipitation Climatology Centre Full Data Reanalysis	gauge	1°/daily	1988 - present	<u>Schamm et al. (2015)</u>
IMERG Early Run	Global Precipitation Measurement Climate Prediction Center – United States	satellite	0.1°/daily	2014 - present	<u>Hou et al. (2014)</u>
CPC	Gauge-based rainfall dataset –Italy	gauge	0.5°/daily	1948 - present	<u>https://www.esrl.noaa.gov/psd/data/gridded/data.unified.daily.conus.html</u>
ITA-DPC	Australian Water Availability Project – Australia	gauge	0.1°/daily	2008 - present	<u>Ciabatta et al. (2017)</u>
AWAP	India Meteorological Department - India	gauge	0.05°/daily	1900 - present	<u>http://www.bom.gov.au/jsp/awap/rain/index.jsp</u>
IMD					<u>http://www.imd.gov.in/pages/services_hydromet.php</u>
SOIL TEMPERATURE and EVAPOTRANSPIRATION					
ERA5	ECMWF	reanalysis	0.25°/daily	1979 - present	<u>https://cds.climate.copernicus.eu/cdsapp#!/dataset/reanalysis-era5-single-levels?tab=overview</u>

731 **Table 2.** Configurations used in the paper (SWI: Soil Water Index, BCO: Brooks-Corey, VGE:
732 van Genuchten, MUA: Mualem-van Genuchten, SWI-Tvar: SWI with T varying with soil
733 moisture, WAV: wavelet filtering, CDF: climatological correction with daily cumulative
734 density function matching, MON: climatological correction with monthly correction factors).

Short Name	Filtering	Losses	Evapotranspiration	Depth varying	Climatological Correction
REF	SWI	BCO	no	no	no
SWI-Tvar	SWI-Tvar	BCO	no	no	no
WAV	WAV	BCO	no	no	no
VGEN	SWI	VGE	no	no	no
MUA	MUA	VGE	no	no	no
EVAP	SWI	BCO	yes	no	no
ZVAR	SWI	BCO	no	yes	no
BC-CDF	SWI-Tvar	BCO	no	no	CDF
BC-MON	SWI-Tvar	BCO	no	no	MON

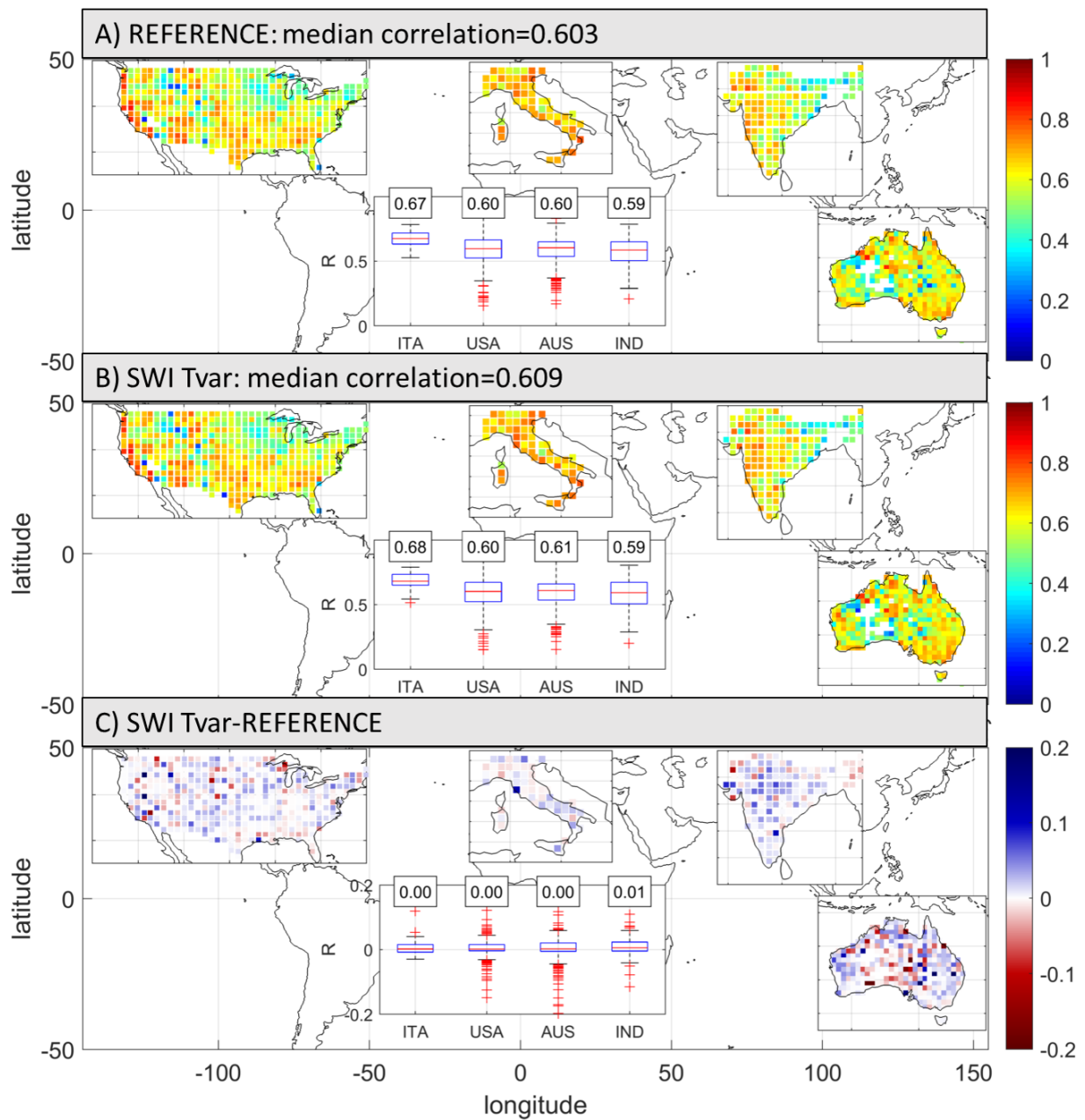
735



737

738 **Figure 1.** Processing steps for obtaining the SM2RAIN-ASCAT global rainfall data record
 739 (2007-2018) from ASCAT surface soil moisture data: pre-processing, SM2RAIN algorithm,
 740 and post-processing. Each bullet represents a possible configuration that has been tested, the
 741 selected configuration is in red, bold font.

742



743

744 **Figure 2.** Performance of two different configurations at 1009 points in terms of Pearson's
 745 correlation, R [-]. A) R map with reference configuration, B) R map with Soil Water Index
 746 (SWI) filtering with variable T as a function of soil moisture, and C) R map difference (B)-(A).
 747 The inner box plots show the R values (and R differences) split for different regions.

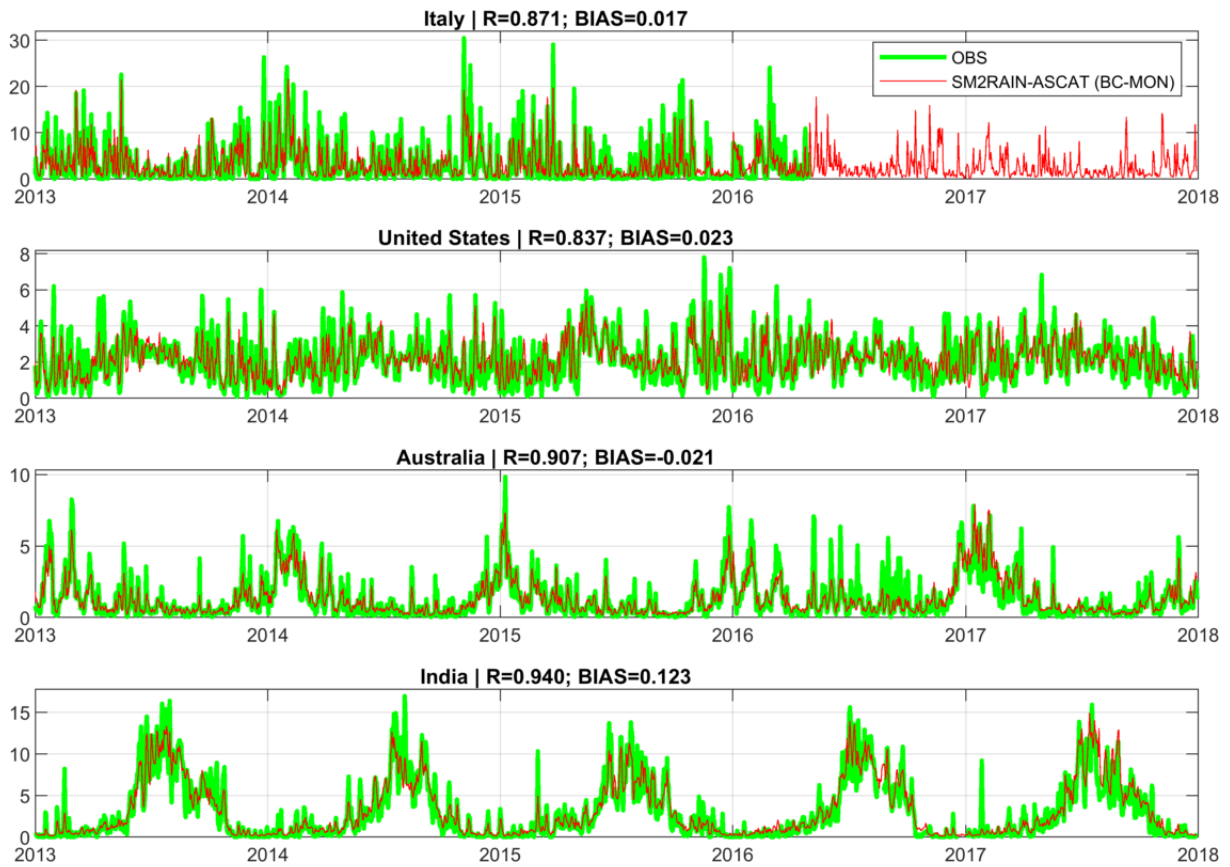
748



749

750 **Figure 3.** Performances at 1009 points in terms of Pearson’s correlation, R [-], root mean square
 751 error, RMSE [mm/day], variability ratio, STDRATIO [-], BIAS [mm/day], false alarm ratio,
 752 FAR [-], Probability of Detection, POD [-], and Threat Score, TS [-]. For details of the different
 753 configurations see Table 2 (GPM-ER: GPM IMERG Early Run product).

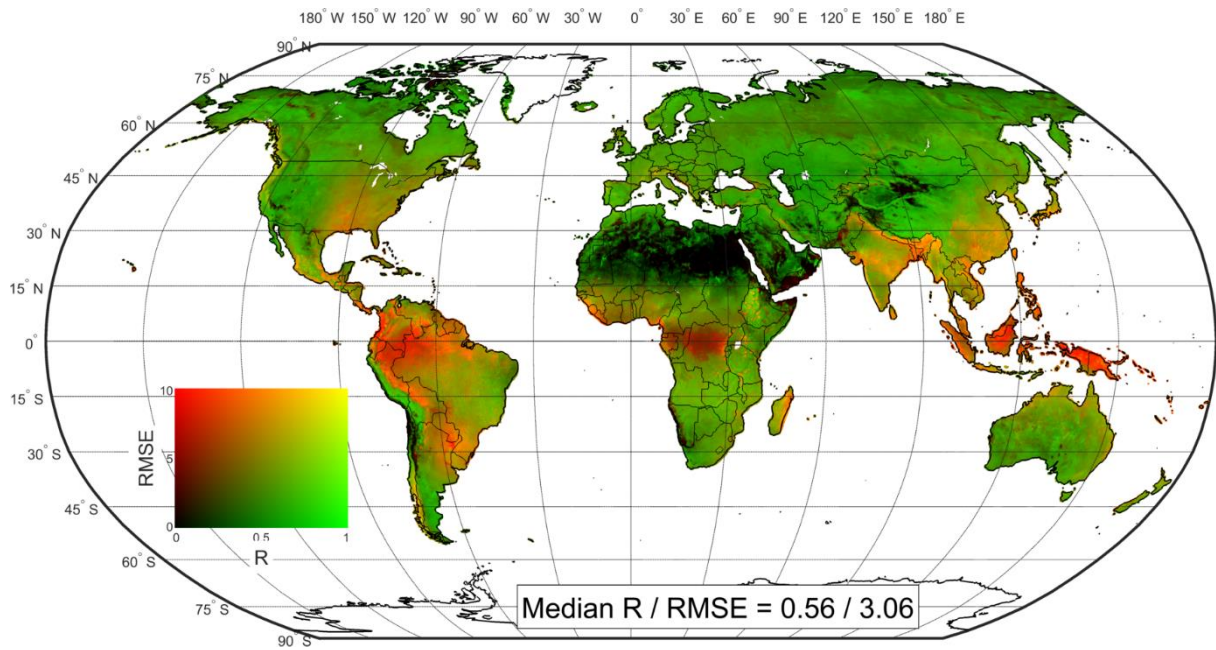
754



755

756 **Figure 4.** Time series of mean areal rainfall for the four regions for observed data, OBS, and
 757 SM2RAIN-ASCAT data record, BC-MON configuration (R [-]: Pearson's correlation, BIAS
 758 [mm/day]: mean error).

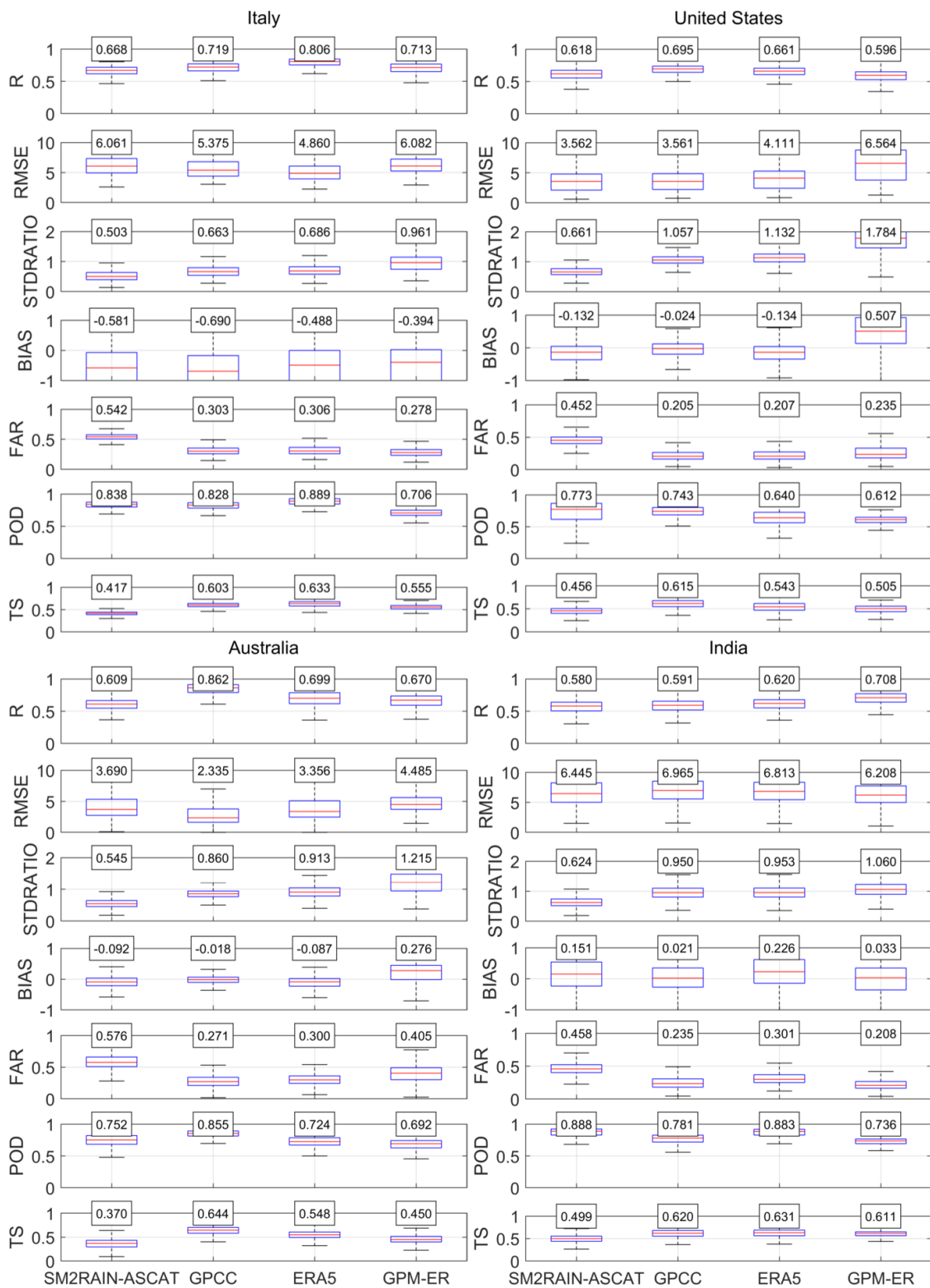
759



760

761 **Figure 5.** Pearson's correlation, R, and root mean square error, RMSE, map of SM2RAIN-
 762 ASCAT data record compared with ERA5 reanalysis dataset used as benchmark (period 2007-
 763 2018). The analysis is carried out at 1-day and 12.5 km temporal and spatial resolution. The
 764 map shows that SM2RAIN-ASCAT data record is performing well in the western United States,
 765 Brazil, southern and western South America, southern Africa, Sahel, southern-central Eurasia,
 766 and Australia (green colours).

767



768

769

770

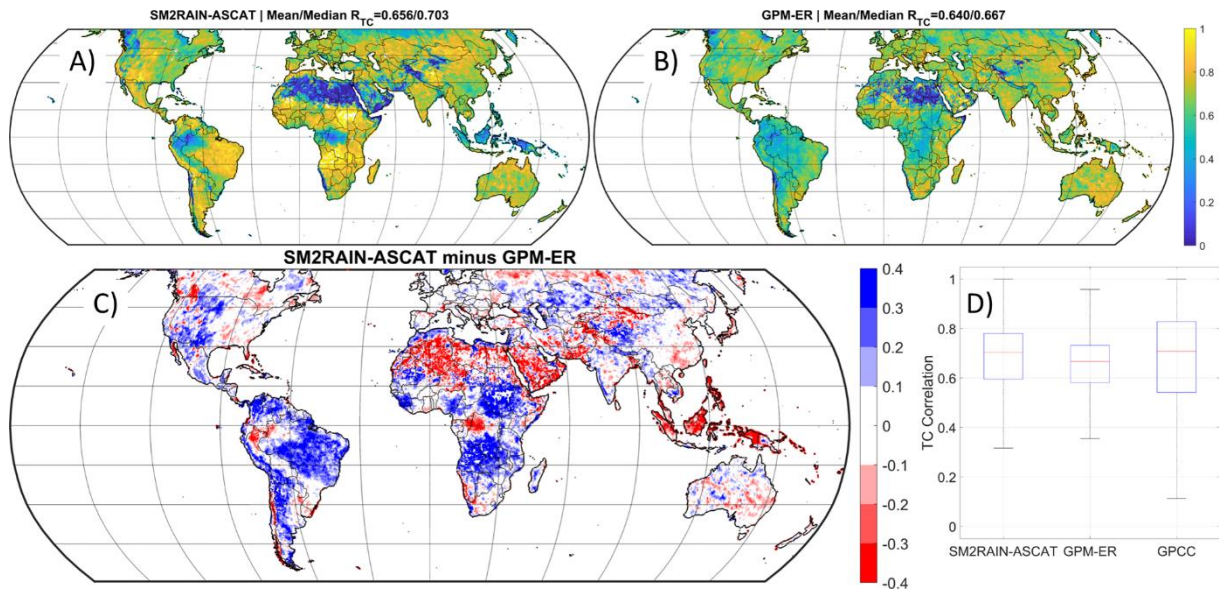
771

772

773

774

Figure 6. Regional assessment of SM2RAIN-ASCAT rainfall data record and comparison with GPCP, ERA5 and GPM-ER rainfall products. As reference the high-quality ground-based datasets in Italy, United States, India and Australia are used. Results in terms of Pearson's correlation, R [-], root mean square error, RMSE [mm/day], variability ratio, STDRATIO [-], BIAS [mm/day], false alarm ratio, FAR [-], Probability of Detection, POD [-], and Threat Score, TS [-].

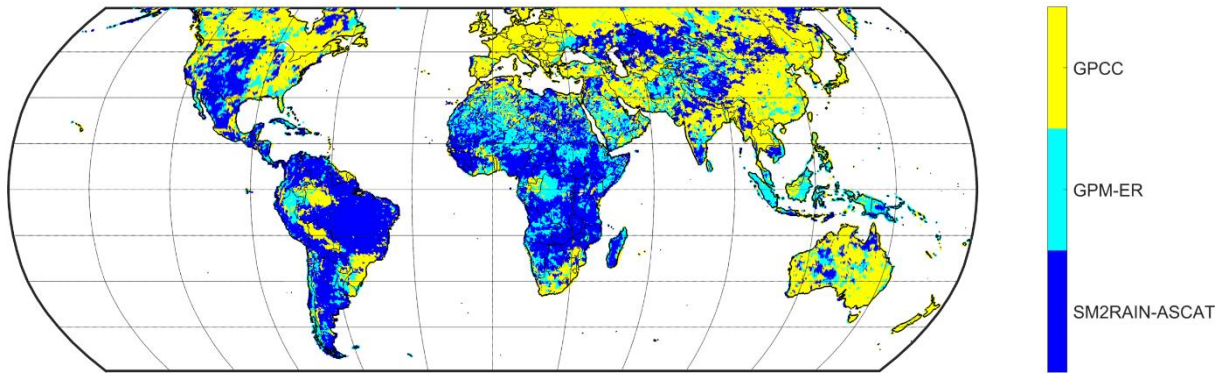


775

776 **Figure 7.** Global triple collocation, TC, results. A) R_{TC} map for SM2RAIN-ASCAT, B) R_{TC}
 777 map for GPM-ER, (C) differences between (A) and (B), i.e., blue (red) colours for pixels in
 778 which SM2RAIN-ASCAT (GPM-ER) is performing better, and D) box plot of R_{TC} for
 779 SM2RAIN-ASCAT, GPM-ER, and GPC. SM2RAIN-ASCAT is performing significantly
 780 better than GPM-ER in South America and Africa (excluding desert and tropical forest areas),
 781 elsewhere the two satellite products perform similarly.

782

783



784

785

786

787

788

789

790

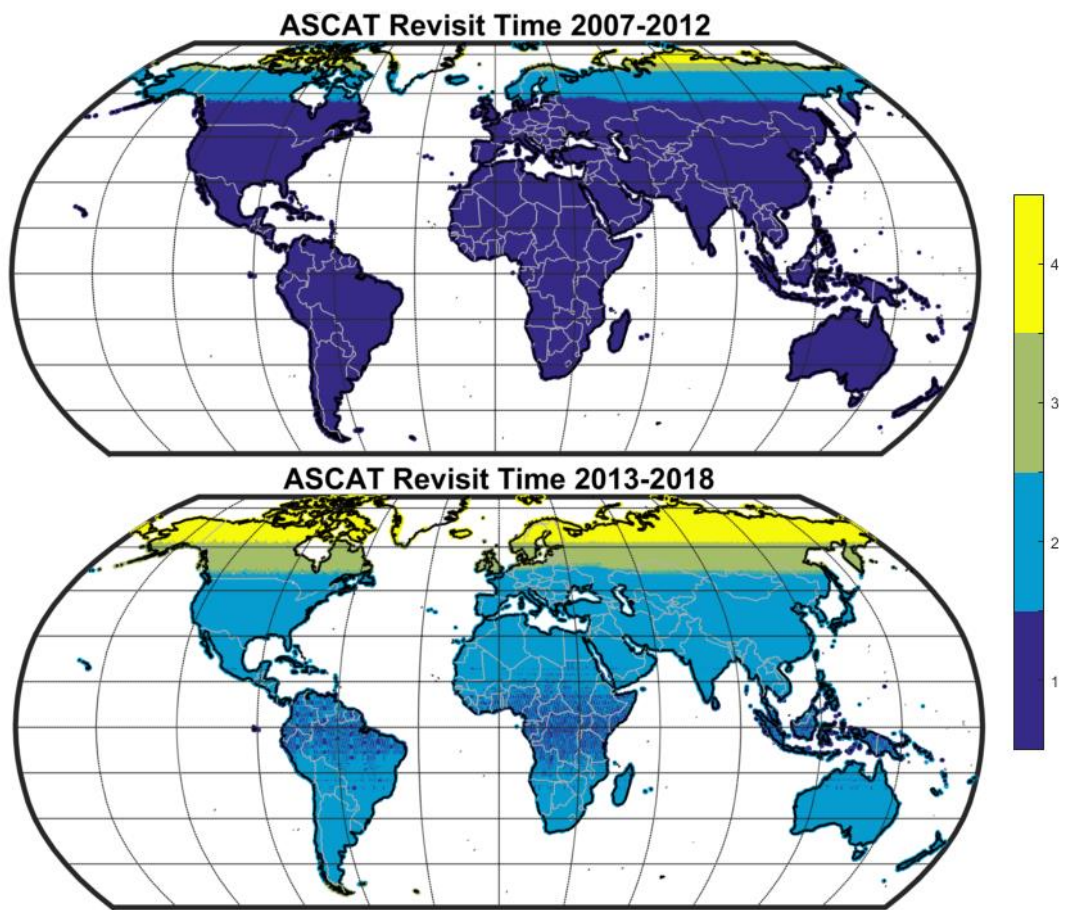
Figure 8. Best performing product based on the results of triple collocation shown in Figure 7. SM2RAIN-ASCAT is performing the best among the three products in Africa, South America, central-western United States and central Asia while GPC is performing the best in the remaining parts of the northern hemisphere and in Australia. GPM-ER is the best product in the tropical and equatorial region.

791 **Appendix**

792 **Table A1.** Equations used for the performance scores. For the continuous scores, P_{ref} is the
 793 reference dataset (e.g., ground observations, ERA5) and P_{est} is the estimated dataset (e.g.,
 794 SM2RAIN-ASCAT, GPM-ER), cov is the covariance operator, σ is the standard deviation
 795 operator, Σ is the summation operator, and N is the sample size. For the categorical scores, H
 796 is the number of successfully predicted events by a given rainfall product, F the number of non-
 797 events erroneously predicted to occur, and M the number of actual events that are missed.

Performance Score	Score symbol	Equation
Continuous scores		
Pearson's correlation	R	$R = \frac{cov(P_{est}, P_{ref})}{\sigma(P_{est})\sigma(P_{ref})}$
Root Mean Square Error	RMSE	$RMSE = \sqrt{\frac{\Sigma(P_{est} - P_{ref})^2}{N}}$
Temporal Variability Ratio	STDRATIO	$STDRATIO = \frac{\sigma(P_{est})}{\sigma(P_{ref})}$
Bias	BIAS	$BIAS = \frac{\Sigma(P_{est} - P_{ref})}{N}$
Categorical scores		
False Alarm Ratio	FAR	$FAR = \frac{F}{H + F}$
Probability of Detection	POD	$POD = \frac{H}{H + M}$
Threat Score	TS	$TS = \frac{H}{H + F + M}$

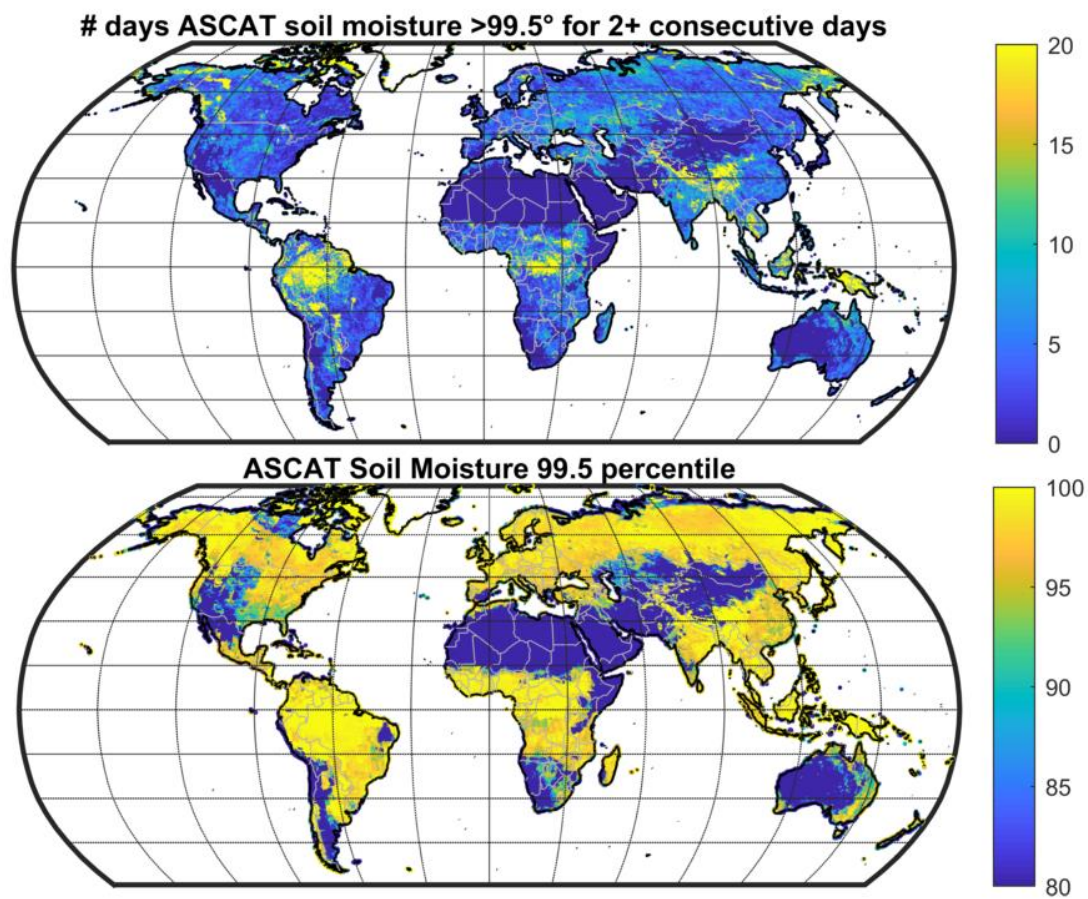
798



799

800 **Figure A1.** Mean daily revisit time [days] of ASCAT soil moisture observations for the period
 801 2007-2012 (only Metop-A, top panel) and for the period 2013-2018 (Metop-A+B, bottom
 802 panel).

803



804

805 **Figure A2.** Number of days in which ASCAT soil moisture observations are close to saturation
 806 (>99.5 percentile, top panel) for 2 (or more) consecutive days in the period 2007-2018. Please
 807 note that the upper value is set to 20 days as in most of land areas the occurrence is very low
 808 (90% of land pixel with values lower than 12 days over 12 years). In the bottom panel the soil
 809 moisture values at 99.5 percentile (in the period 2007-2018) are shown.